ULSAN NATIONAL INSTITUTE OF SCIENCE AND TECHNOLOGY

Master's Thesis

Excited electron dynamics in the 2H-1T heterophase of monolayer MoS_2: time dependent density functional theory study for photo-catalytic mechanism process

Min Choi

Department of Chemistry

Graduate School of UNIST

2017

ULSAN NATIONAL INSTITUTE OF SCIENCE AND TECHNOLOGY

Excited electron dynamics in the 2H-1T heterophase of monolayer MoS_2: time dependent density functional theory study for photo-catalytic mechanism process

Min Choi

Department of Chemistry

Graduate School of UNIST

ULSAN NATIONAL INSTITUTE OF SCIENCE AND TECHNOLOGY

Excited electron dynamics in the 2H-1T heterophase of monolayer MoS_2: time dependent density functional theory study for photo-catalytic mechanism process

A thesis/dissertation
submitted to the Graduate School of UNIST
in partial fulfillment of the
requirements for the degree of
Master of Science

Min Choi

12. 12. 2016
Approved by

_____

Advisor
Noejung Park

Excited electron dynamics in the 2H-1T heterophase of monolayer MoS_2: time dependent density functional theory study for photo-catalytic mechanism process

Min Choi

This certifies that the thesis/dissertation of Min Choi is approved.

12/12/2016

signature

_____

Advisor: Noejung Park

signature

_____

Jino Im: Thesis Committee Member #1

signature

_____

Junhee Lee : Thesis Committee Member #2

Contents

Ⅰ. List of figures ----------1

Ⅱ. List of tables ----------8

Ⅲ. Introduction ----------9

Ⅳ. Computational Details ----------11

Ⅴ. Results

5.A ----------12

5.B ----------13

5.C ----------14

Ⅵ. Conclusion ----------16

List of Figures

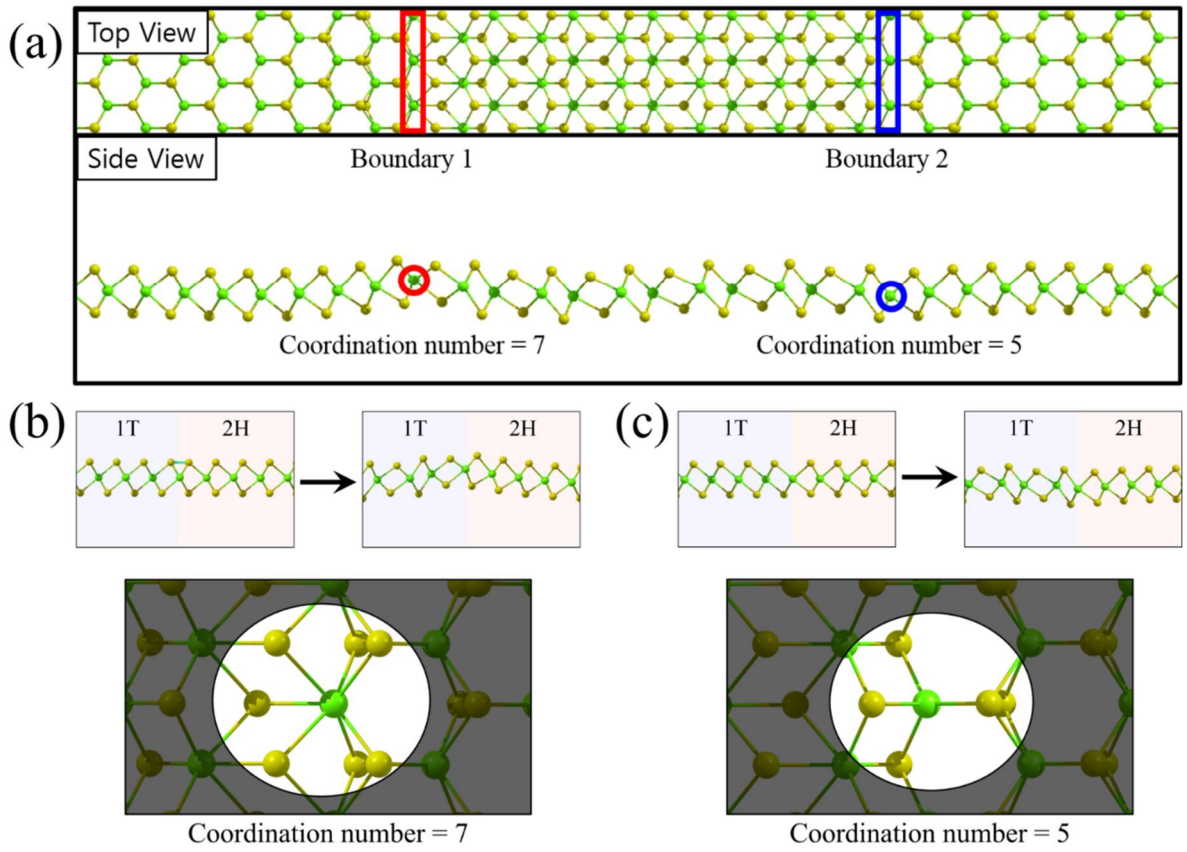

Figure 1 (a) Geometric configuration for 2H-1T heterophase, and the enlarged configurations for (b) 7-fold CN and (c) 5-fold CN boundaries. The green and yellow balls indicate the molybdenum and sulfur atom, respectively.

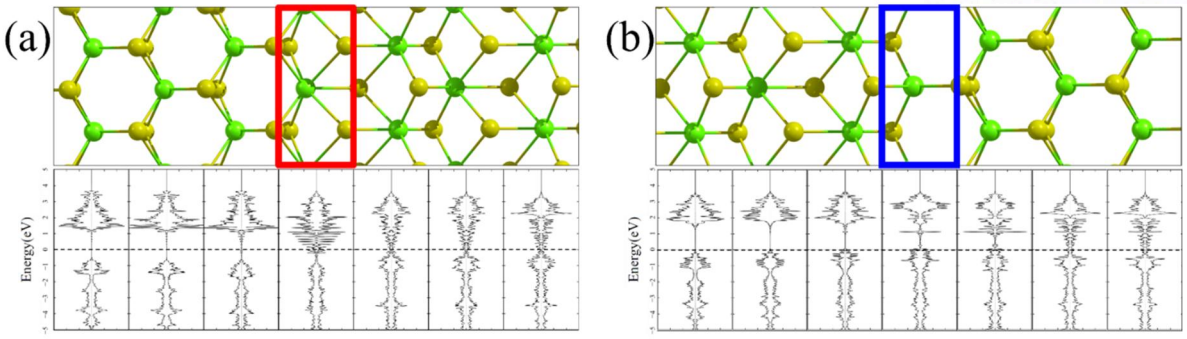

Figure 2 The line density of states (LDOS) for (a) 7-fold CN and (b) 5-fold CN boundaries. The dashed line of LDOS plot guides for the fermi energy level.

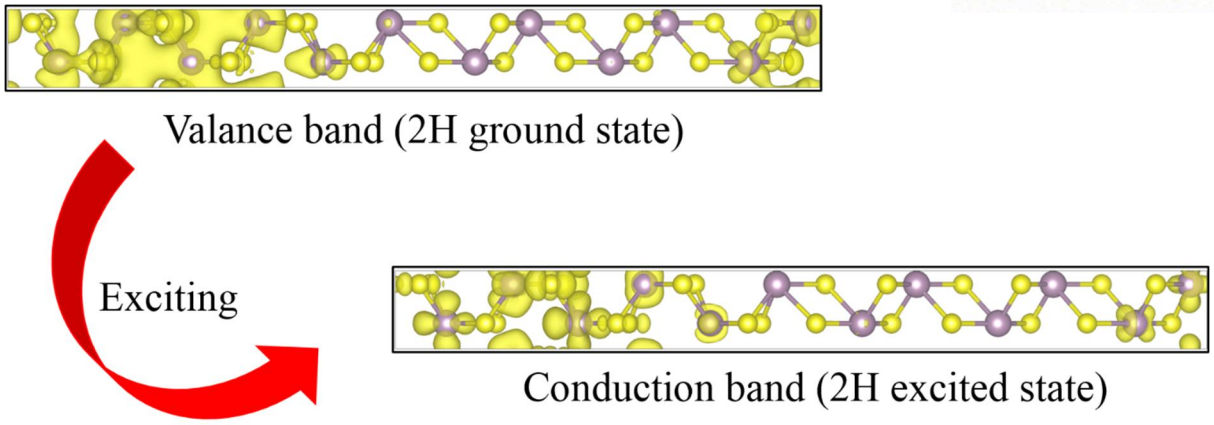

Figure 3 The schematic configuration for electron photo-excitation from valance band maximum (VBM) to conduction band minimum (CBM)

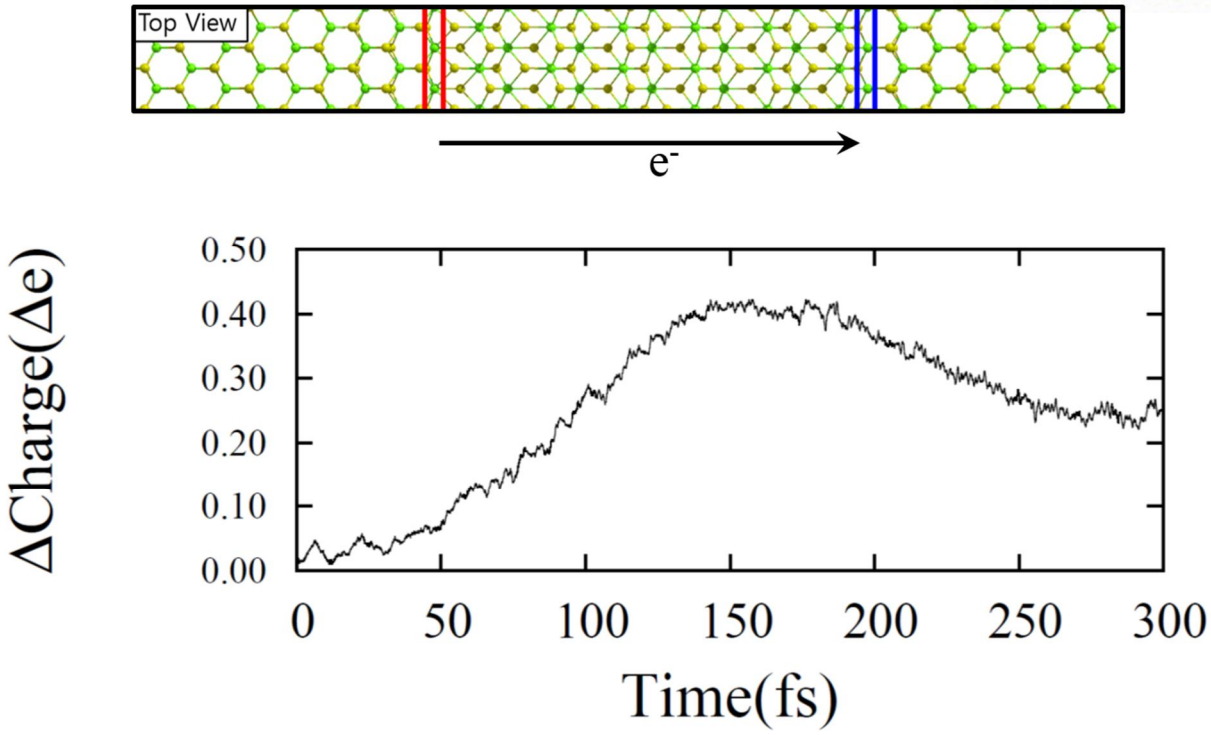

Figure 4 The schematic representation of charge flux direction (upper) and charge difference plot for 1T phase region (lower)

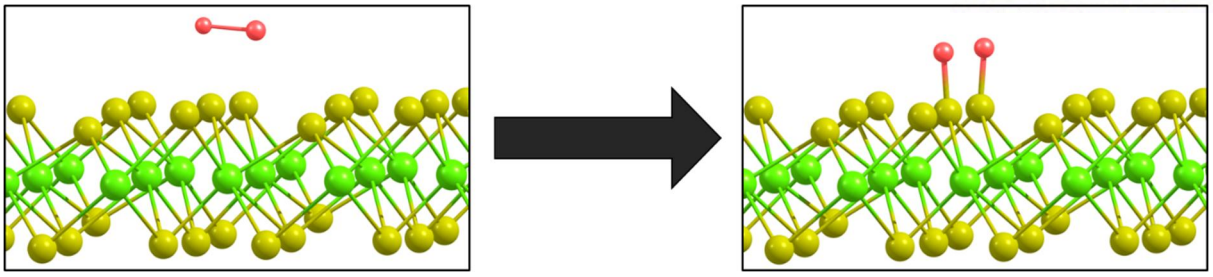

Figure 5 The configurations of initial and final state for oxygen adsorption

Figure 6 The dissociative adsorption energy barrier for basal 1T (left) and charged 1T (right)

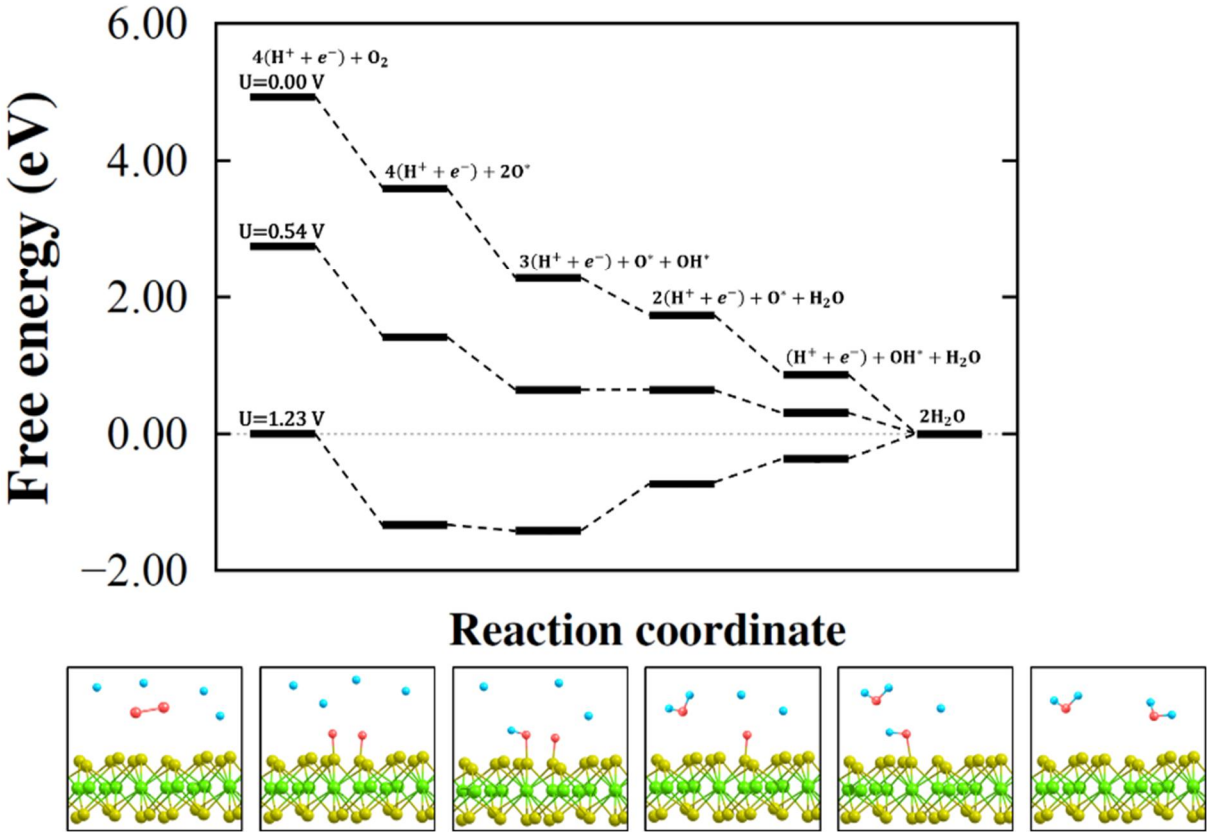

Figure 7 Free-energy profile for oxygen reduction reaction on the charged 1T phase. Results are shown at zero cell potential (U=0V), at the equilibrium potential (U=1.23V), and at the highest potential (U=0.54V) where all reaction steps are exothermic.

List of tables

Table 1 The Results for Bader charge analysis at neutron 1T and charged 1T (2 additional electrons/super-cell).

Bader Charge Analysis	1T	Charged 1T
Before oxygen adsorption		
Mo	+1.254	+1.250
S	-0.6269	-0.6806
O_2	0.00	0.00
After oxygen adsorption		
Mo	+1.237	+1.236
S	-0.5142	-0.5675
O_2	-3.76	-3.81

1. Introduction

Low-dimensional materials, especially transition metal dichalcogenide (TMD), have attracted significant interest these days. The composition of TMD materials is MX_2, where M is transition metal such as Mo and X is chalcogenide molecule such as S. The TMD materials can have two different phases, 2H and 1T, as the stacking positions of chalcogenide molecules. 2H and 1T phase of TMD have trigonal prismatic point group symmetry (D_{3h}) and octahedral point group symmetry (O_h), respectively. Because of these differences of symmetry and the d-orbital splitting of transition metal, TMD materials can show various physical properties such as semiconductor, metal, paramagnetic, antiferromagnetic, and so on.[1,2]

Monolayer MoS_2, one of TMD materials, also shows different physical features as the phases. The 2H phase of MoS_2 is a semiconductor with direct band gap about 2.4 eV, and the 1T phase of MoS_2 has meta-stable metallic phase. The 2H phase of MoS_2 has been studied as a hydrogen evolution reaction (HER) catalyst because of its photovoltaic and photo-catalytic features.[3] On the other hand, the 1T phase of MoS_2 has been investigated in the perspective of nanoscale electronic device, such as ultrathin transistor and supercapacitor electrode component.[4,5,6]

When one electron is injected into the 2H phase of MoS_2, the occupation of E' state of D_{3h} point group is increased. This change of occupation is energetically unstable comparing with the half-filled T_{2g} level of O_h point group. Thus, the phase transition from the 2H phase to 1T phase can occur. Experimentally, Yimin Kang et al. have investigated the phase transition by using the plasmonic hot electron from the deposited Ag nanoparticle on the MoS_2 monolayer.[7] Also, M. A. Py et al. have studied the lithium intercalation method in layered MoS_2 and its phase transition.[8] Goki Eda et al. have observed the structure of mixed phase of MoS_2 by measuring adsorption spectra during lithium intercalation process.[9] They observed the 2H-1T heterophase structure by using high resolution scanning transmission electron microscopy (HR-STEM), and Yung-Chang Lin et al. have investigated the atomic mechanism of this phase transition phenomena.[10,11] Theoretically, Xiaoyan Guo et al. have calculated the electronic properties, especially density of state, of the interface of MoS_2 2H-1T heterophase.[12] However, the detail researches about 2H-1T heterophase such as boundary structure, electron dynamics, and electron transfer between 2H and 1T phase are still unclear.

In this study, we investigated geometric and electronic structure of the MoS_2 heterophase. We found that two different types of phase boundary lead to difference in the band alignments at MoS_2 phase

boundaries. As a consequence, the excited electrons in the 2H phase region are transferred and accumulated in the 1T phase region, leading to the charging of the 1T phase region. We performed the real-time time dependent density functional theory (rt-TDDFT) calculation for this electron dynamics. We found that, as the 1T phase is charged, the activation barrier of dissociative adsorption of oxygen molecule on the planar surface of 1T phase is decreased. In the acidic condition, the oxygen reduction reaction (ORR) energy profile on the charged 1T phase region shows similar electrochemical properties with that on the platinum (100) surface. We suggest that the MoS_2 heterophase can serve as the novel low-dimensional ORR photo-catalyst.

2. Computation Details

A. Electronic and geometric structure

To perform the first-principle calculations, we used the Vienna Ab initio Simulation Package (VASP) source code. For the exchange-correlation potential, a plane-wave basis set with an energy cutoff of 450 eV and the Perdew-Burke-Ernzerhof (PBE) type gradient-correlated functional were employed. The atomic pseudopotentials were described with the Projector Augmented Wave (PAW) method, as provided with the aforementioned package. The heterophase structure was composed with 1x12 rectangular cell of 2H phase and that of 1T phase. The x-direction lattice mismatch between 2H and 1T phase was 0.2%, thus we attached the two rectangular cells along the y-direction. The k-point grids for the heterophase structure were sampled 1x20x1 by using the scheme of the Monkhorst-Pack.

B. Activation energy

The 4x4 1T phase hexagonal supercell with 3x3x1 k-point grids sampling by using the same scheme was employed to investigate the activation barrier of dissociative adsorption of oxygen molecule as the charge accumulation in 1T phase. The nudged elastic band (NEB) method was used to calculate the activation barriers.

C. Oxygen reduction reaction

We assume that $H^+ + e^-$ is in equilibrium with $\frac{1}{2}H_2$, at pH 0 and 0V versus the standard hydrogen electrode (SHE). The free energy of water in the liquid phase was estimated as,

$$G_{H_2O(l)} = G_{H_2O(g)} + RT\ln(\frac{p}{p_0})$$

Where R is the gas constant, T=300K, p=0.035 bar, and p_0=1bar. The free energy of the H^+ ion was derived as

$$G_{H^+(aq)} = \frac{1}{2}G_{H_2(g)} - RT\ln 10 \times \mathrm{pH}$$

In the acidic condition, O_2 is reduced as $O_2 + 4H^+ + 4e^- \rightarrow 2H_2O$, where the elementary reaction steps on the catalytic surface are

1. $O_2(g) + 4H^+(aq) + 4e^- + 2* \rightarrow 2O^* + 4H^+(aq) + 4e^-$
2. $2O^* + 4H^+(aq) + 4e^- \rightarrow O^* + OH^* + 3H^+(aq) + 3e^-$
3. $O^* + OH^* + 3H^+(aq) + 3e^- \rightarrow O^* + H_2O(l) + 2H^+(aq) + 2e^-$
4. $O^* + H_2O(l) + 2H^+(aq) + 2e^- \rightarrow OH^* + H_2O(l) + H^+(aq) + e^-$
5. $OH^* + H_2O(l) + H^+(aq) + e^- \rightarrow 2H_2O(l)$

Where * denotes the free surface, and $H_2O(l)$ indicates liquid water.

3. Result

3.1 Geometric & Electronic Structure

The super-cell what we calculated is consisting of 1x12x1 rectangular cell of 2H and 1T structures. We arranged the rectangular 2H and 1T phase along the y-axis like Figure-1(a), and the lattice mismatch between 2H and 1T phase is 0.42%. The O_h point group, Mo point group of 1T phase, has inversion symmetry while D_{3h} point group, Mo point group of 2H phase, does not. For that reason, there are two different types of boundary, 5-fold and 7-fold coordination number (CN) of transition metal, when the 2H-1T heterophase is formed. Geometrically, the steric effect of 7-fold CN of transition metal is increased because the basal CN of transition metal of TMD materials is 6-fold. In Figure-1(b), therefore, the 7-fold CN boundary has ripple while 5-fold CN boundary is flat.

This change of geometry influences in the electronic structures of the boundaries. When the CN of transition metal is increased from 6-fold to 7-fold, the added chalcogen atom, sulfur for MoS_2 case, increases the oxidation number of transition metal. Thus, the transition metal at the 7-fold CN boundary has more state above the fermi level. On the other hand, the transition metal at the 5-fold CN boundary has less state above the fermi level because the oxidation number of 5-fold CN of transition metal is decreased. For that reason, the electron can be transferred from 7-fold CN boundary to 5-fold CN boundary.

3.2 Excited electron dynamics

We calculated the electron dynamics when photo-excitation occurs at the 2H phase region of aforementioned 2H-1T heterophase structure by using real-time time dependent density functional theory (rt-TDDFT). To decrease the calculating cost for rt-TDDFT calculation, we truncated the 2H-1T heterophase structure in half along the y-axis, so the calculated structure is consisting on the 1x6x1 2H phase and 1x6x1 1T phase. As depicted in the Figure 3, we excite an electron pair from the valance band maximum (VBM) to the conduction band minimum (CBM).

As the schematic configuration in Figure-4(a), the excited electron pair at the 2H phase region is transferred to 1T phase region by passing through the 7-fold CN boundary. Thus, we integrated the charge density at the only 1T phase region by using the following equation,

$$Q_{transferred}(t) = \int_{last\ \mathrm{Mo_{1T}}}^{first\ \mathrm{Mo_{1T}}} \rho(\boldsymbol{r}, t) d\boldsymbol{r},$$

and the transferred charge versus time is plotted in Figure-4(b). The charge density at 1T phase region is increased because the excited charge flows into the 1T phase region via 7-fold CN boundary. As time goes by, the amount of transferred charge has been increased until the excited carrier reaching to the 5-fold CN boundary. After the excited electron passing the 5-fold CN boundary, the amount of transferred charge starts to be decreased. Thus, the retention time for the excited charge staying in the 1T phase region is determined by the size of 1T phase region. For the calculated structure, the 0.4 electrons transferred to 1x6x1 1T phase region, therefore, the $0.067\ electons/_{MoS_{2\,UnitCell}}$ is transferred from 2H phase region to 1T phase region when the electron pair is excited from the 2H phase VBM.

3.3 Application for oxygen reduction reaction

Aforementioned phenomena represent that the 1T phase region is instantaneously charged when the exciton is generated at the 2H phase region. The charged surface can be utilized for various fields, and the application as the catalyst for oxygen reduction reaction (ORR) is one of them. Several researches have been reported that the charged system or electron applied system such as nitrogen doped graphene or Cabrera-Mott model insulator improve the ORR properties.[13,14] We have studied the ORR properties of the charged 1T phase based on these researches by using DFT calculation.

As described schematic configuration in Figure-5, we calculated the binding energy of oxygen molecule on the 3x3x1 rectangular 1T phase supercell. The oxygen molecule is dissociated and adsorbed on the sulfur atom of 1T phase MoS2, and the binding energy is 0.723eV by following equation,

$$E_{Binding} = \frac{1}{2}\left[E_{MoS_2+O_2} - \{E_{MoS_2} + E_{O_2}\}\right].$$

The oxygen molecule should be dissociative adsorbed on the 1T phase MoS2 thermodynamically, however that phenomena does not be happened in real. Thus, we calculated the activation energy for dissociative adsorption ($E_{a_{diss}}$) by using the nudged elastic band (NEB) method as implemented with the VASP code, and considered the kinetical component based on the Arrhenius type reaction rate.

As depicted in Figure-6, the $E_{a_{diss}}$ on the basal 1T phase is about 2.5eV, and it is extremely high barrier comparing with Boltzmann factor at room temperature, about 0.026eV. However, $E_{a_{diss}}$ is decreased dramatically when the ORR system is charged. Especially, the $E_{a_{diss}}$ is decreased to 0.05eV when $0.067\ electons/_{MoS_{2_{UnitCell}}}$, the result of our rt-TDDFT calculation, is charged at the 1T phase.

Also, we calculated the Bader charge analysis to study the reason why $E_{a_{diss}}$ is dramatically decreased as the additional charge. As the Table-1 shown, the charge at molybdenum atom is not changed when the excess charge is injected. The charge at sulfur atom, however, is increased as same amount of the excess charge. The charge at molybdenum atom is still not changed when oxygen molecule is adsorbed while the charge at sulfur atom is decreased. That is, the excess charge deposits in only sulfur atom, the outer layer of MoS_2, and that charge transfers to oxygen molecule for dissociative adsorption. Therefore, the electron affinity of oxygen molecule helps to decrease $E_{a_{diss}}$ by being dragged to the charged surface of MoS_2.

Herein, we utilize the dissociative adsorbed oxygen molecule on the 1T phase MoS_2 as following steps

for 4-electron the ORR mechanism.

$O_2 + 4H^+ + 4e^- \rightarrow 2O^* + 4H^+ + e^-$

$2O^* + 4H^+ + 4e^- \rightarrow O^* + HO^* + 3H^+ + 3e^-$

$O^* + HO^* + 3H^+ + 3e^- \rightarrow O^* + H_2O + 2H^+ + 2e^-$

$O^* + H_2O + 2H^+ + 2e^- \rightarrow HO^* + H_2O + H^+ + e^-$

$HO^* + H_2O + H^+ + e^- \rightarrow 2H_2O$

Based on the standard hydrogen electrode, the potential for oxygen molecule reduction, $O_2 + 4H^+ \rightarrow 2H_2O$, is 1.23V when the potential for protonation of hydrogen molecule is 0V. In the Figure-7, the free-energy diagram by calculating the potentials for each electron transfer step based on the free-energy calculation method of Norskov et al. shows that the potential profile has downhill until overpotential, μ, is 0.54V, and after that the potential profile has uphill.[15] That is, the current has not been changed until the bias potential reaching from 0V to 0.54V. But after the μ over the 0.54V, the current is decreased because of uphill at the free-energy diagram following the Butler-Volmer equation,

$i_k = i_0 e^{(U/kT)}$.

4. Conclusion

The 2H-1T heterophase can has two-type boundaries as the CN of transition metal at the boundary. The CN of transition metal can influence in the geometric and electronic structure of that heterophase, and it decides the direction of electron transfer from 2H phase to 1T phase. The amount of transferred electron is $0.067\ electons/_{MoS_{2\,UnitCell}}$ and it's enough to attract oxygen molecule onto the 1T phase of MoS_2 with extremely decreased adsorption activation energy. The dissociative adsorption of oxygen molecule is rate determine step (RDS) for ORR mechanism, and this photovoltaic effect at 2H phase of MoS_2 supports to improve the ORR properties on the 1T phase of MoS_2. Our results of free-energy diagram shows that the maximum overpotential where the proton transfer step is down-hill in energy is 0.54V. Experimentally, the ORR property, especially i-v curve data, on Pt (100) surface shows similar result with ours.[16] From our simulation results, the electron transfer from 2H, the semiconductor phase, to 1T, the metallic phase, by photovoltaic effect can improve the ORR property and it be utilized as the photo-catalyst for ORR.

REFERENCES

1. Manish Chhowalla, Hyeon Suk Shin, Goki Eda, Lain-Jong Li, Kian Ping Loh, and Hua Zhang; Nature Chemistry (2013) vol 5 263-275

2. Andrey N. Enyashin, Lena Yadgarov, Lothar Houben, Igor Popov, Marc Weidenbash ReshefTenne, Maya Bar-Sadan, and Gotthard Seifert; The Journal of Physical Chemicsry C (2011) 155, 24586-24591

3. Haotian Wang, Zhiyi Lu, Shicheng Xu, Desheng Kong, Judy J. Cha, Guangyuan Zheng, Po-Chun Hsu, Kai Yan, David Bradshaw, Fritz B. Prinz, and Yi Cui; Proceeding of th eNational Academy of Sciences of the United States of America (PNAS) (2013) 110, 19701-19706

4. Muharrem Acerce, Damien Voiry, and Manish Chhowalla; Nature Nanotechnology (2015) 10, 313-318

5. Xiao Huang, Zhiyuan Zeng, and Hua Zhang; Chem. Soc. Rev. (2013) 42, 1934-1946

6. Rajesh Kappera, Damien Voiry, Sibel Ebru Yalcin, Brittany Branch, Gautam Gupta, Aditya D. Mohite, and Manish Chhowalla; Nature Materials (2014) vol 13 1128-1134

7. Yimin Kang, Sina Najmaei, Zheng Liu, Yanjun Bao, Yumin Wang, Xing Zhu, Naomi J. Halas, Peter Nordlander, Pulickel M. Ajayan, Jun Lou, and Zheyu Fang; Advanced Materials (2014) 26 6467-6471

8. M. A. Py, R. R. Haering; Canadian Journal of Physics (1983) 61, 76-84

9. Goki Eda, Hisato Yamaguchi, Damien Voiry, Takeshi Fujita, Mingwei Chen, and Manish Chhowalla; Nano Letter (2011) 11, 5111-5116

10. Goki Eda, Takeshi Fujita, Hisato Yamaguchi, Damien Voiry, Mingwei Chen, and Manish Chhowalla; ACS Nano (2012) vol 6 7311-7317

11. Yung-Chang Lin, Dumitru O. Dumcenco, Ying-Sheng Huang, and Kazu Suenaga; Nature Nanotechnology (2014) vol 9 391-396

12. Xiaoyan Guo, Guihui Yang, Junfeng Zhang, and Xiaohong Xu; AIP Advances (2015) 5, 097174

13. Linfer Lai, Jeffrey R. Potts, Da Zhan, Liang Wang, Chee Kok Poh, Chunhua Tang, Hao Gong, Zexiang Shen, Jianyi Lin, and Rodney S. Ruoff; Energy Envitonment Science (2012) 5, 7936-7942

14. Dongbin Shin, S. Sinthika, Min Choi, Ranjit Thapa, Noejung Park; ACS Catalyst (2014) 4, 4074-4080

15. Origin of the Overpotential for Oxygen Reduction at a Fuel-Cell Cathode
J.K. Norskov, J. Rossmeisl, A. Logadottir, L. Lindqvist, J. R. Kitchin, T. Bligaard, and H. Jonsson; J. Phys. Chem. B (2004) 108, 17886-17892

16. N.M.Markovic, P.N.Ross Jr.; Surface Science Reports 45 (2002) 117-229

Master's Thesis

Excited electron dynamics in the 2H-1T heterophase of monolayer MoS_2: time dependent density functional theory study for photo-catalytic mechanism process

Min Choi

Department of Chemistry

Graduate School of UNIST

2017

Excited electron dynamics in the 2H-1T heterophase of monolayer MoS_2: time dependent density functional theory study for photo-catalytic mechanism process

Min Choi

Department of Chemistry

Graduate School of UNIST

Excited electron dynamics in the 2H-1T heterophase of monolayer MoS_2: time dependent density functional theory study for photo-catalytic mechanism process

A thesis/dissertation
submitted to the Graduate School of UNIST
in partial fulfillment of the
requirements for the degree of
Master of Science

Min Choi

12. 12. 2016
Approved by

_____

Advisor
Noejung Park

Excited electron dynamics in the 2H-1T heterophase of monolayer MoS_2: time dependent density functional theory study for photo-catalytic mechanism process

Min Choi

This certifies that the thesis/dissertation of Min Choi is approved.

12/12/2016

signature

_____

Advisor: Noejung Park

signature

_____

Jino Im: Thesis Committee Member #1

signature

_____

Junhee Lee : Thesis Committee Member #2

Contents

Ⅰ. List of figures ----------1

Ⅱ. List of tables ----------8

Ⅲ. Introduction ----------9

Ⅳ. Computational Details ----------11

Ⅴ. Results

5.A ----------12

5.B ----------13

5.C ----------14

Ⅵ. Conclusion ----------16

List of Figures

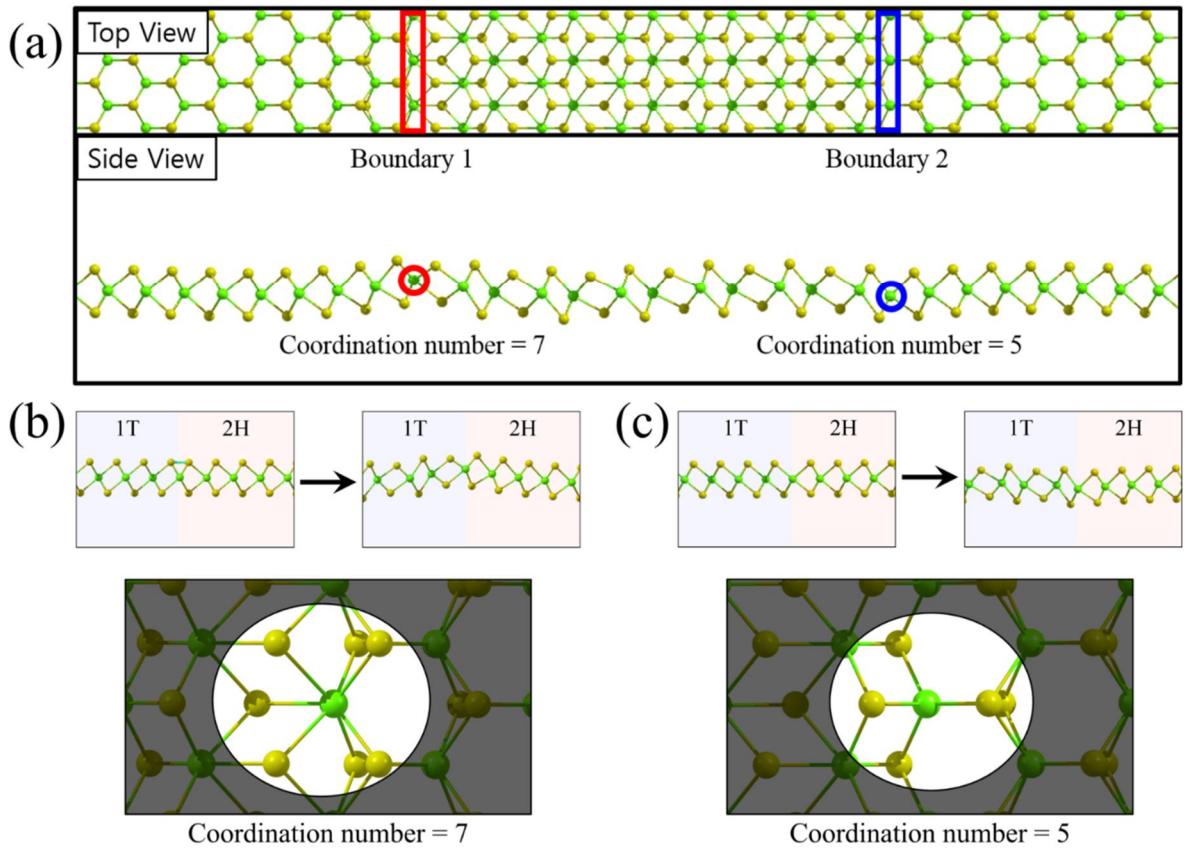

Figure 1 (a) Geometric configuration for 2H-1T heterophase, and the enlarged configurations for (b) 7-fold CN and (c) 5-fold CN boundaries. The green and yellow balls indicate the molybdenum and sulfur atom, respectively.

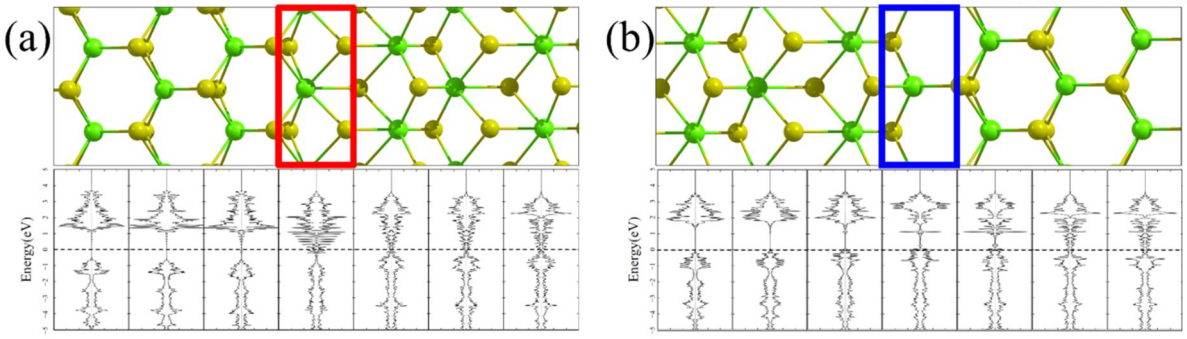

Figure 2 The line density of states (LDOS) for (a) 7-fold CN and (b) 5-fold CN boundaries. The dashed line of LDOS plot guides for the fermi energy level.

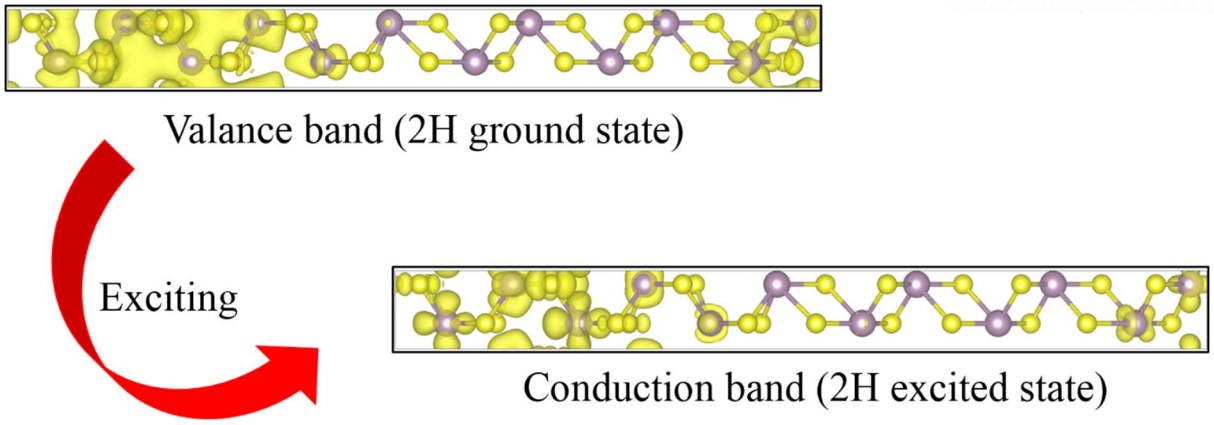

Figure 3 The schematic configuration for electron photo-excitation from valance band maximum (VBM) to conduction band minimum (CBM)

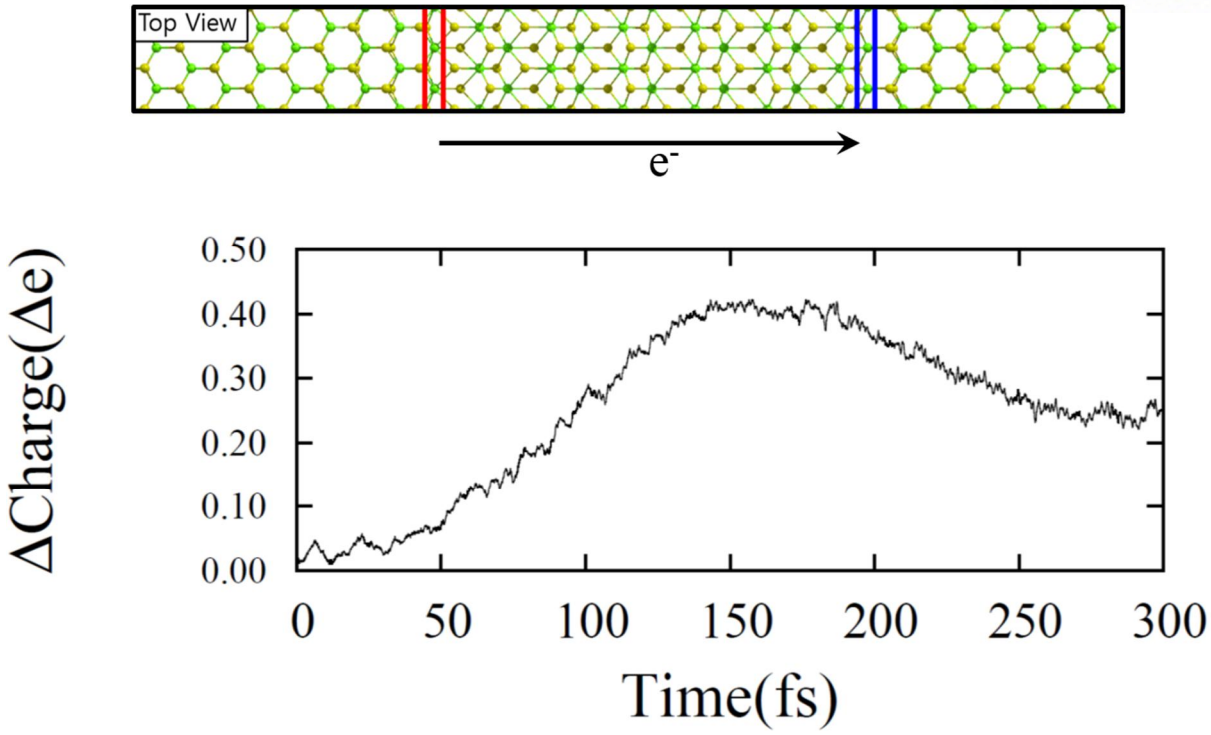

Figure 4 The schematic representation of charge flux direction (upper) and charge difference plot for 1T phase region (lower)

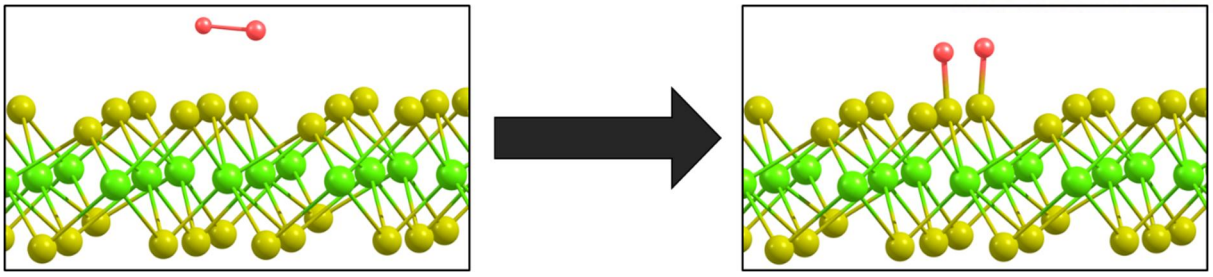

Figure 5 The configurations of initial and final state for oxygen adsorption

Figure 6 The dissociative adsorption energy barrier for basal 1T (left) and charged 1T (right)

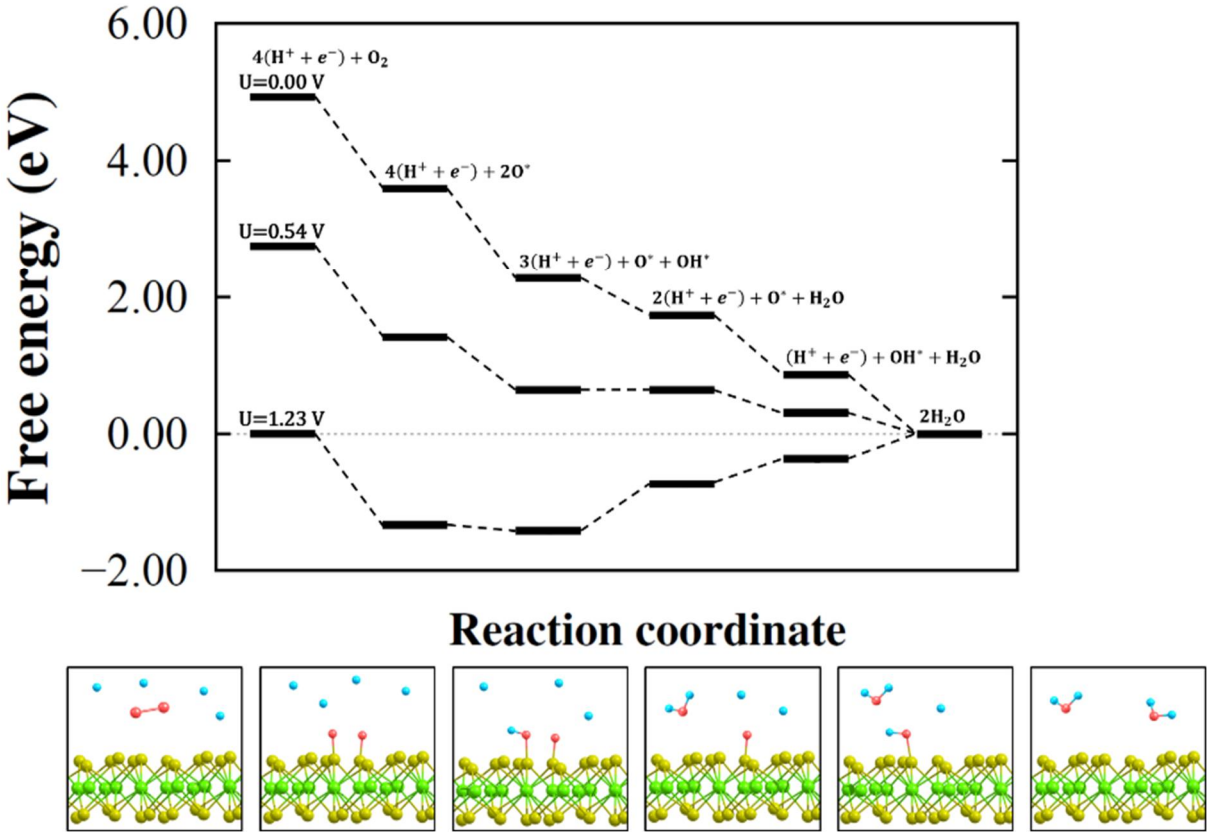

Figure 7 Free-energy profile for oxygen reduction reaction on the charged 1T phase. Results are shown at zero cell potential (U=0V), at the equilibrium potential (U=1.23V), and at the highest potential (U=0.54V) where all reaction steps are exothermic.

List of tables

Table 1 The Results for Bader charge analysis at neutron 1T and charged 1T (2 additional electrons/super-cell).

Bader Charge Analysis	1T	Charged 1T
Before oxygen adsorption		
Mo	+1.254	+1.250
S	-0.6269	-0.6806
O_2	0.00	0.00
After oxygen adsorption		
Mo	+1.237	+1.236
S	-0.5142	-0.5675
O_2	-3.76	-3.81

1. Introduction

Low-dimensional materials, especially transition metal dichalcogenide (TMD), have attracted significant interest these days. The composition of TMD materials is MX_2, where M is transition metal such as Mo and X is chalcogenide molecule such as S. The TMD materials can have two different phases, 2H and 1T, as the stacking positions of chalcogenide molecules. 2H and 1T phase of TMD have trigonal prismatic point group symmetry (D_{3h}) and octahedral point group symmetry (O_h), respectively. Because of these differences of symmetry and the d-orbital splitting of transition metal, TMD materials can show various physical properties such as semiconductor, metal, paramagnetic, antiferromagnetic, and so on.[1,2]

Monolayer MoS_2, one of TMD materials, also shows different physical features as the phases. The 2H phase of MoS_2 is a semiconductor with direct band gap about 2.4 eV, and the 1T phase of MoS_2 has meta-stable metallic phase. The 2H phase of MoS_2 has been studied as a hydrogen evolution reaction (HER) catalyst because of its photovoltaic and photo-catalytic features.[3] On the other hand, the 1T phase of MoS_2 has been investigated in the perspective of nanoscale electronic device, such as ultrathin transistor and supercapacitor electrode component.[4,5,6]

When one electron is injected into the 2H phase of MoS_2, the occupation of E' state of D_{3h} point group is increased. This change of occupation is energetically unstable comparing with the half-filled T_{2g} level of O_h point group. Thus, the phase transition from the 2H phase to 1T phase can occur. Experimentally, Yimin Kang et al. have investigated the phase transition by using the plasmonic hot electron from the deposited Ag nanoparticle on the MoS_2 monolayer.[7] Also, M. A. Py et al. have studied the lithium intercalation method in layered MoS_2 and its phase transition.[8] Goki Eda et al. have observed the structure of mixed phase of MoS_2 by measuring adsorption spectra during lithium intercalation process.[9] They observed the 2H-1T heterophase structure by using high resolution scanning transmission electron microscopy (HR-STEM), and Yung-Chang Lin et al. have investigated the atomic mechanism of this phase transition phenomena.[10,11] Theoretically, Xiaoyan Guo et al. have calculated the electronic properties, especially density of state, of the interface of MoS_2 2H-1T heterophase.[12] However, the detail researches about 2H-1T heterophase such as boundary structure, electron dynamics, and electron transfer between 2H and 1T phase are still unclear.

In this study, we investigated geometric and electronic structure of the MoS_2 heterophase. We found that two different types of phase boundary lead to difference in the band alignments at MoS_2 phase

boundaries. As a consequence, the excited electrons in the 2H phase region are transferred and accumulated in the 1T phase region, leading to the charging of the 1T phase region. We performed the real-time time dependent density functional theory (rt-TDDFT) calculation for this electron dynamics. We found that, as the 1T phase is charged, the activation barrier of dissociative adsorption of oxygen molecule on the planar surface of 1T phase is decreased. In the acidic condition, the oxygen reduction reaction (ORR) energy profile on the charged 1T phase region shows similar electrochemical properties with that on the platinum (100) surface. We suggest that the MoS_2 heterophase can serve as the novel low-dimensional ORR photo-catalyst.

2. Computation Details

A. Electronic and geometric structure

To perform the first-principle calculations, we used the Vienna Ab initio Simulation Package (VASP) source code. For the exchange-correlation potential, a plane-wave basis set with an energy cutoff of 450 eV and the Perdew-Burke-Ernzerhof (PBE) type gradient-correlated functional were employed. The atomic pseudopotentials were described with the Projector Augmented Wave (PAW) method, as provided with the aforementioned package. The heterophase structure was composed with 1x12 rectangular cell of 2H phase and that of 1T phase. The x-direction lattice mismatch between 2H and 1T phase was 0.2%, thus we attached the two rectangular cells along the y-direction. The k-point grids for the heterophase structure were sampled 1x20x1 by using the scheme of the Monkhorst-Pack.

B. Activation energy

The 4x4 1T phase hexagonal supercell with 3x3x1 k-point grids sampling by using the same scheme was employed to investigate the activation barrier of dissociative adsorption of oxygen molecule as the charge accumulation in 1T phase. The nudged elastic band (NEB) method was used to calculate the activation barriers.

C. Oxygen reduction reaction

We assume that $H^+ + e^-$ is in equilibrium with $\frac{1}{2}H_2$, at pH 0 and 0V versus the standard hydrogen electrode (SHE). The free energy of water in the liquid phase was estimated as,

$$G_{H_2O(l)} = G_{H_2O(g)} + RT\ln(\frac{p}{p_0})$$

Where R is the gas constant, T=300K, p=0.035 bar, and p_0=1bar. The free energy of the H^+ ion was derived as

$$G_{H^+(aq)} = \frac{1}{2}G_{H_2(g)} - RT\ln 10 \times \mathrm{pH}$$

In the acidic condition, O_2 is reduced as $O_2 + 4H^+ + 4e^- \rightarrow 2H_2O$, where the elementary reaction steps on the catalytic surface are

1. $O_2(g) + 4H^+(aq) + 4e^- + 2* \rightarrow 2O^* + 4H^+(aq) + 4e^-$
2. $2O^* + 4H^+(aq) + 4e^- \rightarrow O^* + OH^* + 3H^+(aq) + 3e^-$
3. $O^* + OH^* + 3H^+(aq) + 3e^- \rightarrow O^* + H_2O(l) + 2H^+(aq) + 2e^-$
4. $O^* + H_2O(l) + 2H^+(aq) + 2e^- \rightarrow OH^* + H_2O(l) + H^+(aq) + e^-$
5. $OH^* + H_2O(l) + H^+(aq) + e^- \rightarrow 2H_2O(l)$

Where * denotes the free surface, and $H_2O(l)$ indicates liquid water.

3. Result

3.1 Geometric & Electronic Structure

The super-cell what we calculated is consisting of 1x12x1 rectangular cell of 2H and 1T structures. We arranged the rectangular 2H and 1T phase along the y-axis like Figure-1(a), and the lattice mismatch between 2H and 1T phase is 0.42%. The O_h point group, Mo point group of 1T phase, has inversion symmetry while D_{3h} point group, Mo point group of 2H phase, does not. For that reason, there are two different types of boundary, 5-fold and 7-fold coordination number (CN) of transition metal, when the 2H-1T heterophase is formed. Geometrically, the steric effect of 7-fold CN of transition metal is increased because the basal CN of transition metal of TMD materials is 6-fold. In Figure-1(b), therefore, the 7-fold CN boundary has ripple while 5-fold CN boundary is flat.

This change of geometry influences in the electronic structures of the boundaries. When the CN of transition metal is increased from 6-fold to 7-fold, the added chalcogen atom, sulfur for MoS_2 case, increases the oxidation number of transition metal. Thus, the transition metal at the 7-fold CN boundary has more state above the fermi level. On the other hand, the transition metal at the 5-fold CN boundary has less state above the fermi level because the oxidation number of 5-fold CN of transition metal is decreased. For that reason, the electron can be transferred from 7-fold CN boundary to 5-fold CN boundary.

3.2 Excited electron dynamics

We calculated the electron dynamics when photo-excitation occurs at the 2H phase region of aforementioned 2H-1T heterophase structure by using real-time time dependent density functional theory (rt-TDDFT). To decrease the calculating cost for rt-TDDFT calculation, we truncated the 2H-1T heterophase structure in half along the y-axis, so the calculated structure is consisting on the 1x6x1 2H phase and 1x6x1 1T phase. As depicted in the Figure 3, we excite an electron pair from the valance band maximum (VBM) to the conduction band minimum (CBM).

As the schematic configuration in Figure-4(a), the excited electron pair at the 2H phase region is transferred to 1T phase region by passing through the 7-fold CN boundary. Thus, we integrated the charge density at the only 1T phase region by using the following equation,

$$Q_{transferred}(t) = \int_{last\ \mathrm{Mo_{1T}}}^{first\ \mathrm{Mo_{1T}}} \rho(\boldsymbol{r}, t) d\boldsymbol{r},$$

and the transferred charge versus time is plotted in Figure-4(b). The charge density at 1T phase region is increased because the excited charge flows into the 1T phase region via 7-fold CN boundary. As time goes by, the amount of transferred charge has been increased until the excited carrier reaching to the 5-fold CN boundary. After the excited electron passing the 5-fold CN boundary, the amount of transferred charge starts to be decreased. Thus, the retention time for the excited charge staying in the 1T phase region is determined by the size of 1T phase region. For the calculated structure, the 0.4 electrons transferred to 1x6x1 1T phase region, therefore, the $0.067\ electons/_{MoS_{2_{UnitCell}}}$ is transferred from 2H phase region to 1T phase region when the electron pair is excited from the 2H phase VBM.

3.3 Application for oxygen reduction reaction

Aforementioned phenomena represent that the 1T phase region is instantaneously charged when the exciton is generated at the 2H phase region. The charged surface can be utilized for various fields, and the application as the catalyst for oxygen reduction reaction (ORR) is one of them. Several researches have been reported that the charged system or electron applied system such as nitrogen doped graphene or Cabrera-Mott model insulator improve the ORR properties.[13,14] We have studied the ORR properties of the charged 1T phase based on these researches by using DFT calculation.

As described schematic configuration in Figure-5, we calculated the binding energy of oxygen molecule on the 3x3x1 rectangular 1T phase supercell. The oxygen molecule is dissociated and adsorbed on the sulfur atom of 1T phase MoS2, and the binding energy is 0.723eV by following equation,

$$E_{Binding} = \frac{1}{2}\left[E_{MoS_2+O_2} - \{E_{MoS_2} + E_{O_2}\}\right].$$

The oxygen molecule should be dissociative adsorbed on the 1T phase MoS2 thermodynamically, however that phenomena does not be happened in real. Thus, we calculated the activation energy for dissociative adsorption ($E_{a_{diss}}$) by using the nudged elastic band (NEB) method as implemented with the VASP code, and considered the kinetical component based on the Arrhenius type reaction rate.

As depicted in Figure-6, the $E_{a_{diss}}$ on the basal 1T phase is about 2.5eV, and it is extremely high barrier comparing with Boltzmann factor at room temperature, about 0.026eV. However, $E_{a_{diss}}$ is decreased dramatically when the ORR system is charged. Especially, the $E_{a_{diss}}$ is decreased to 0.05eV when $0.067\ electons/_{MoS_{2_{UnitCell}}}$, the result of our rt-TDDFT calculation, is charged at the 1T phase.

Also, we calculated the Bader charge analysis to study the reason why $E_{a_{diss}}$ is dramatically decreased as the additional charge. As the Table-1 shown, the charge at molybdenum atom is not changed when the excess charge is injected. The charge at sulfur atom, however, is increased as same amount of the excess charge. The charge at molybdenum atom is still not changed when oxygen molecule is adsorbed while the charge at sulfur atom is decreased. That is, the excess charge deposits in only sulfur atom, the outer layer of MoS_2, and that charge transfers to oxygen molecule for dissociative adsorption. Therefore, the electron affinity of oxygen molecule helps to decrease $E_{a_{diss}}$ by being dragged to the charged surface of MoS_2.

Herein, we utilize the dissociative adsorbed oxygen molecule on the 1T phase MoS_2 as following steps

for 4-electron the ORR mechanism.

$O_2 + 4H^+ + 4e^- \rightarrow 2O^* + 4H^+ + e^-$

$2O^* + 4H^+ + 4e^- \rightarrow O^* + HO^* + 3H^+ + 3e^-$

$O^* + HO^* + 3H^+ + 3e^- \rightarrow O^* + H_2O + 2H^+ + 2e^-$

$O^* + H_2O + 2H^+ + 2e^- \rightarrow HO^* + H_2O + H^+ + e^-$

$HO^* + H_2O + H^+ + e^- \rightarrow 2H_2O$

Based on the standard hydrogen electrode, the potential for oxygen molecule reduction, $O_2 + 4H^+ \rightarrow 2H_2O$, is 1.23V when the potential for protonation of hydrogen molecule is 0V. In the Figure-7, the free-energy diagram by calculating the potentials for each electron transfer step based on the free-energy calculation method of Norskov et al. shows that the potential profile has downhill until overpotential, μ, is 0.54V, and after that the potential profile has uphill.[15] That is, the current has not been changed until the bias potential reaching from 0V to 0.54V. But after the μ over the 0.54V, the current is decreased because of uphill at the free-energy diagram following the Butler-Volmer equation,

$i_k = i_0 e^{(U/kT)}$.

4. Conclusion

The 2H-1T heterophase can has two-type boundaries as the CN of transition metal at the boundary. The CN of transition metal can influence in the geometric and electronic structure of that heterophase, and it decides the direction of electron transfer from 2H phase to 1T phase. The amount of transferred electron is $0.067\ electons/_{MoS_{2\,UnitCell}}$ and it's enough to attract oxygen molecule onto the 1T phase of MoS_2 with extremely decreased adsorption activation energy. The dissociative adsorption of oxygen molecule is rate determine step (RDS) for ORR mechanism, and this photovoltaic effect at 2H phase of MoS_2 supports to improve the ORR properties on the 1T phase of MoS_2. Our results of free-energy diagram shows that the maximum overpotential where the proton transfer step is down-hill in energy is 0.54V. Experimentally, the ORR property, especially i-v curve data, on Pt (100) surface shows similar result with ours.[16] From our simulation results, the electron transfer from 2H, the semiconductor phase, to 1T, the metallic phase, by photovoltaic effect can improve the ORR property and it be utilized as the photo-catalyst for ORR.

REFERENCES

1. Manish Chhowalla, Hyeon Suk Shin, Goki Eda, Lain-Jong Li, Kian Ping Loh, and Hua Zhang; Nature Chemistry (2013) vol 5 263-275

2. Andrey N. Enyashin, Lena Yadgarov, Lothar Houben, Igor Popov, Marc Weidenbash ReshefTenne, Maya Bar-Sadan, and Gotthard Seifert; The Journal of Physical Chemicsry C (2011) 155, 24586-24591

3. Haotian Wang, Zhiyi Lu, Shicheng Xu, Desheng Kong, Judy J. Cha, Guangyuan Zheng, Po-Chun Hsu, Kai Yan, David Bradshaw, Fritz B. Prinz, and Yi Cui; Proceeding of th eNational Academy of Sciences of the United States of America (PNAS) (2013) 110, 19701-19706

4. Muharrem Acerce, Damien Voiry, and Manish Chhowalla; Nature Nanotechnology (2015) 10, 313-318

5. Xiao Huang, Zhiyuan Zeng, and Hua Zhang; Chem. Soc. Rev. (2013) 42, 1934-1946

6. Rajesh Kappera, Damien Voiry, Sibel Ebru Yalcin, Brittany Branch, Gautam Gupta, Aditya D. Mohite, and Manish Chhowalla; Nature Materials (2014) vol 13 1128-1134

7. Yimin Kang, Sina Najmaei, Zheng Liu, Yanjun Bao, Yumin Wang, Xing Zhu, Naomi J. Halas, Peter Nordlander, Pulickel M. Ajayan, Jun Lou, and Zheyu Fang; Advanced Materials (2014) 26 6467-6471

8. M. A. Py, R. R. Haering; Canadian Journal of Physics (1983) 61, 76-84

9. Goki Eda, Hisato Yamaguchi, Damien Voiry, Takeshi Fujita, Mingwei Chen, and Manish Chhowalla; Nano Letter (2011) 11, 5111-5116

10. Goki Eda, Takeshi Fujita, Hisato Yamaguchi, Damien Voiry, Mingwei Chen, and Manish Chhowalla; ACS Nano (2012) vol 6 7311-7317

11. Yung-Chang Lin, Dumitru O. Dumcenco, Ying-Sheng Huang, and Kazu Suenaga; Nature Nanotechnology (2014) vol 9 391-396

12. Xiaoyan Guo, Guihui Yang, Junfeng Zhang, and Xiaohong Xu; AIP Advances (2015) 5, 097174

13. Linfer Lai, Jeffrey R. Potts, Da Zhan, Liang Wang, Chee Kok Poh, Chunhua Tang, Hao Gong, Zexiang Shen, Jianyi Lin, and Rodney S. Ruoff; Energy Envitonment Science (2012) 5, 7936-7942

14. Dongbin Shin, S. Sinthika, Min Choi, Ranjit Thapa, Noejung Park; ACS Catalyst (2014) 4, 4074-4080

15. Origin of the Overpotential for Oxygen Reduction at a Fuel-Cell Cathode
J.K. Norskov, J. Rossmeisl, A. Logadottir, L. Lindqvist, J. R. Kitchin, T. Bligaard, and H. Jonsson; J. Phys. Chem. B (2004) 108, 17886-17892

16. N.M.Markovic, P.N.Ross Jr.; Surface Science Reports 45 (2002) 117-229

Master's Thesis

Excited electron dynamics in the 2H-1T heterophase of monolayer MoS_2: time dependent density functional theory study for photo-catalytic mechanism process

Min Choi

Department of Chemistry

Graduate School of UNIST

2017

Excited electron dynamics in the 2H-1T heterophase of monolayer MoS_2: time dependent density functional theory study for photo-catalytic mechanism process

Min Choi

Department of Chemistry

Graduate School of UNIST

Excited electron dynamics in the 2H-1T heterophase of monolayer MoS_2: time dependent density functional theory study for photo-catalytic mechanism process

A thesis/dissertation
submitted to the Graduate School of UNIST
in partial fulfillment of the
requirements for the degree of
Master of Science

Min Choi

12. 12. 2016
Approved by

_____

Advisor
Noejung Park

Excited electron dynamics in the 2H-1T heterophase of monolayer MoS_2: time dependent density functional theory study for photo-catalytic mechanism process

Min Choi

This certifies that the thesis/dissertation of Min Choi is approved.

12/12/2016

signature

_____

Advisor: Noejung Park

signature

_____

Jino Im: Thesis Committee Member #1

signature

_____

Junhee Lee : Thesis Committee Member #2

Contents

Ⅰ. List of figures ----------1

Ⅱ. List of tables ----------8

Ⅲ. Introduction ----------9

Ⅳ. Computational Details ----------11

Ⅴ. Results

5.A ----------12

5.B ----------13

5.C ----------14

Ⅵ. Conclusion ----------16

List of Figures

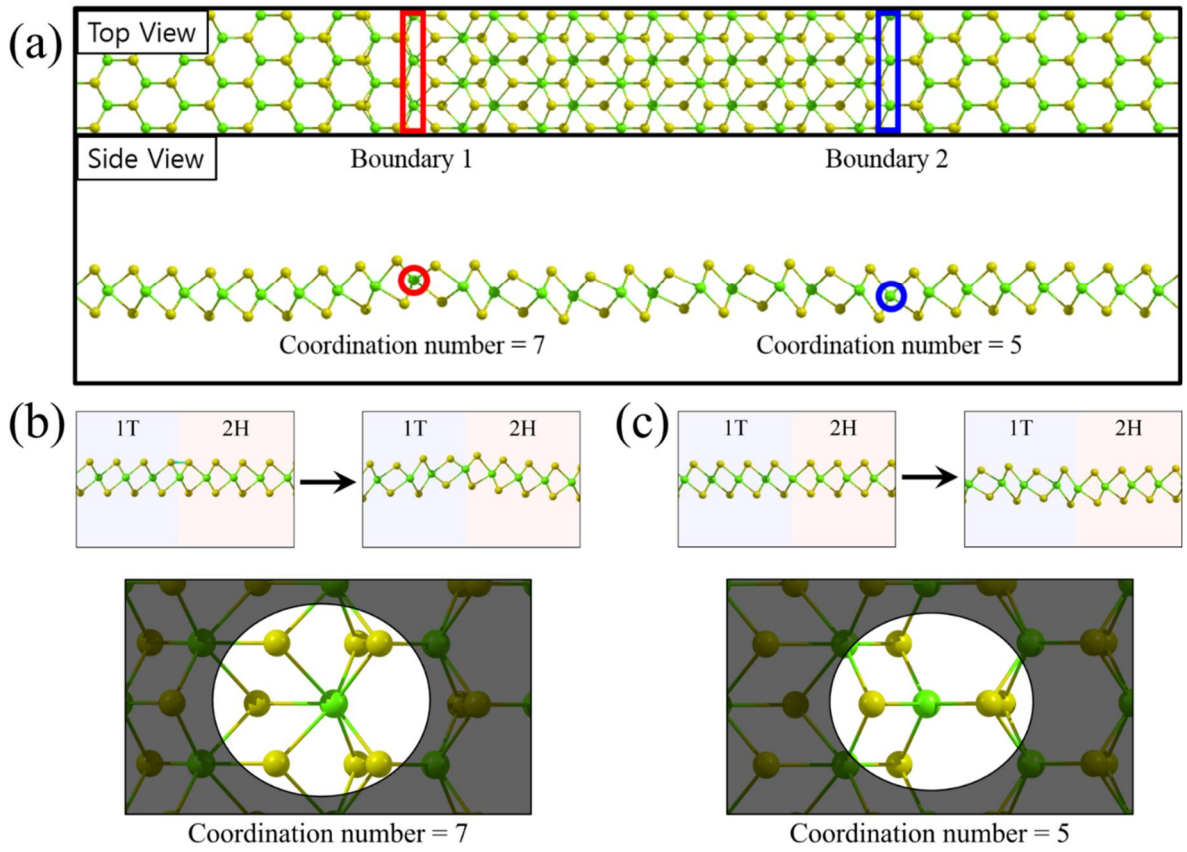

Figure 1 (a) Geometric configuration for 2H-1T heterophase, and the enlarged configurations for (b) 7-fold CN and (c) 5-fold CN boundaries. The green and yellow balls indicate the molybdenum and sulfur atom, respectively.

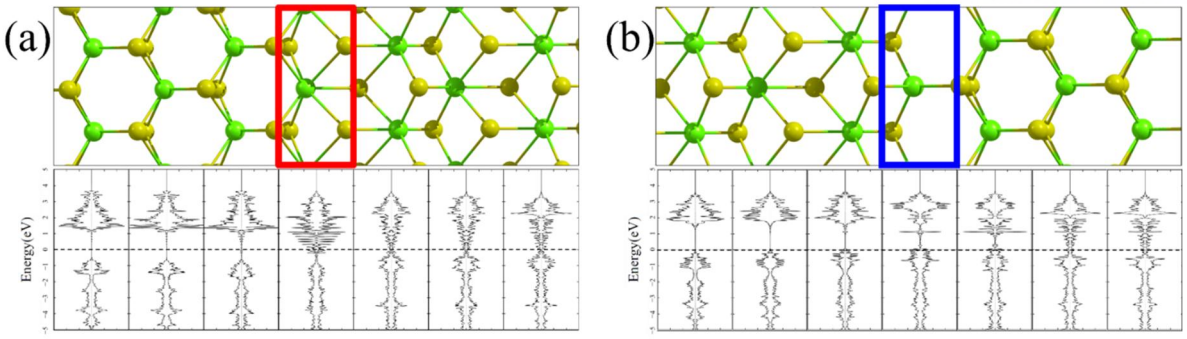

Figure 2 The line density of states (LDOS) for (a) 7-fold CN and (b) 5-fold CN boundaries. The dashed line of LDOS plot guides for the fermi energy level.

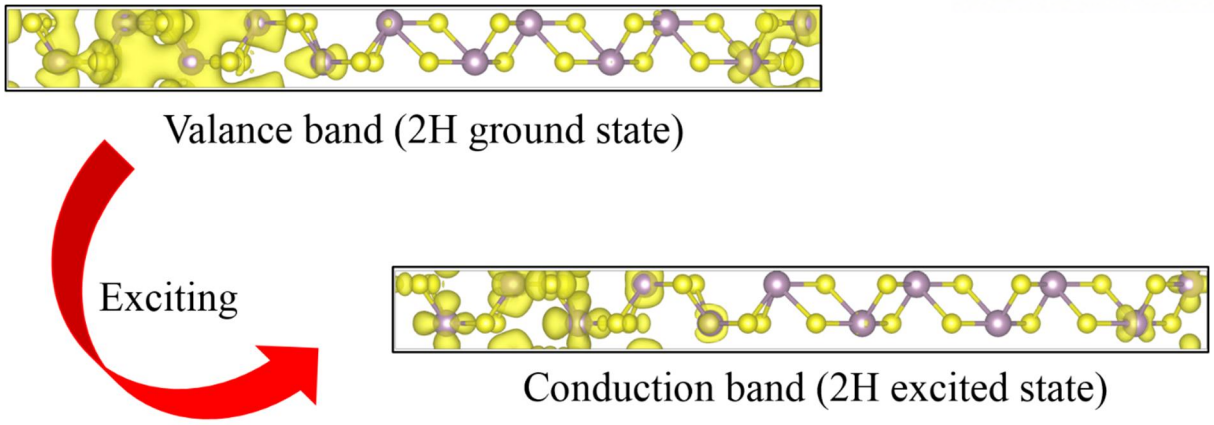

Figure 3 The schematic configuration for electron photo-excitation from valance band maximum (VBM) to conduction band minimum (CBM)

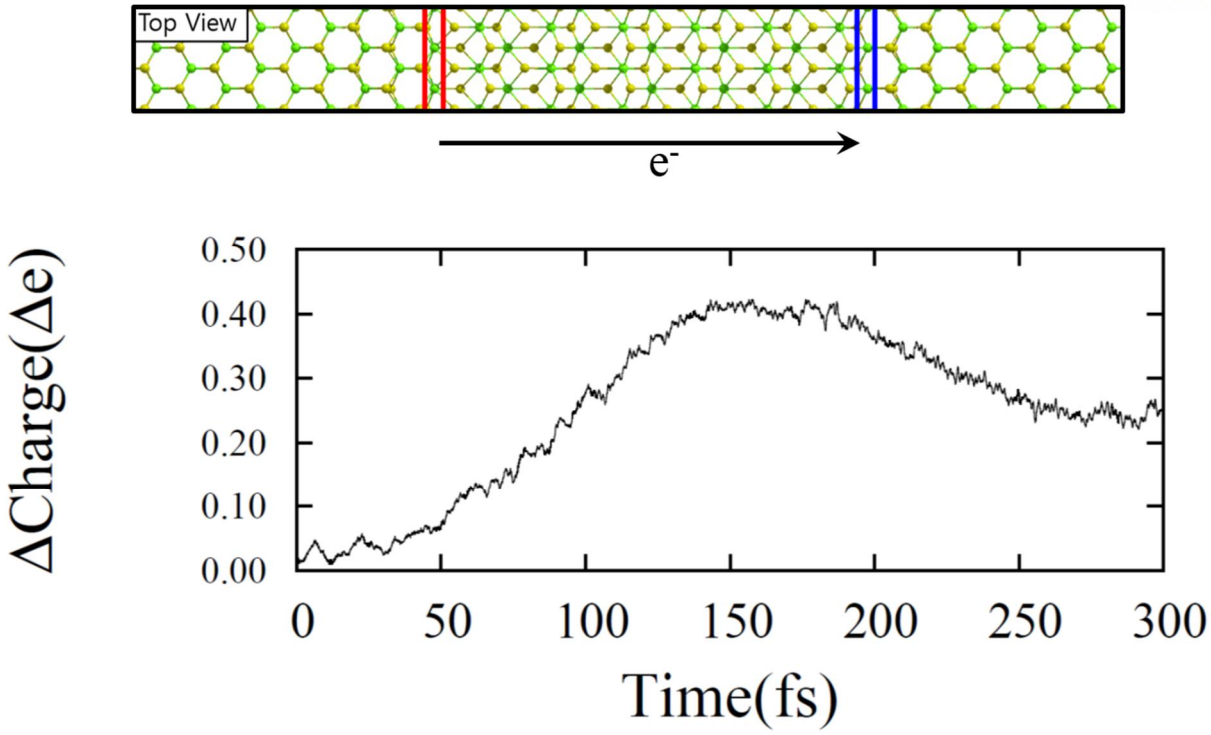

Figure 4 The schematic representation of charge flux direction (upper) and charge difference plot for 1T phase region (lower)

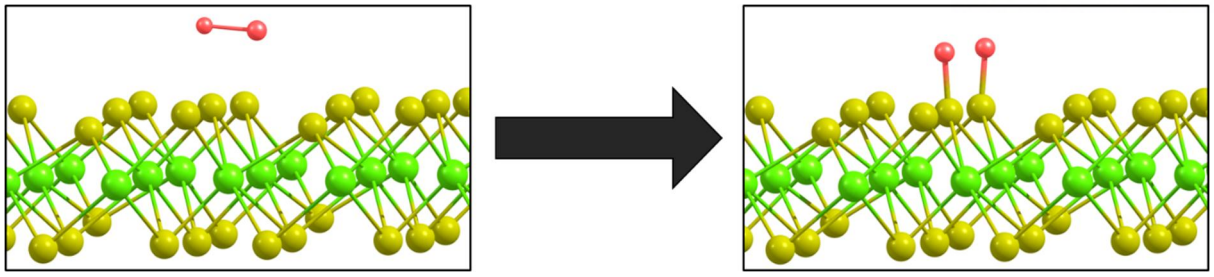

Figure 5 The configurations of initial and final state for oxygen adsorption

Figure 6 The dissociative adsorption energy barrier for basal 1T (left) and charged 1T (right)

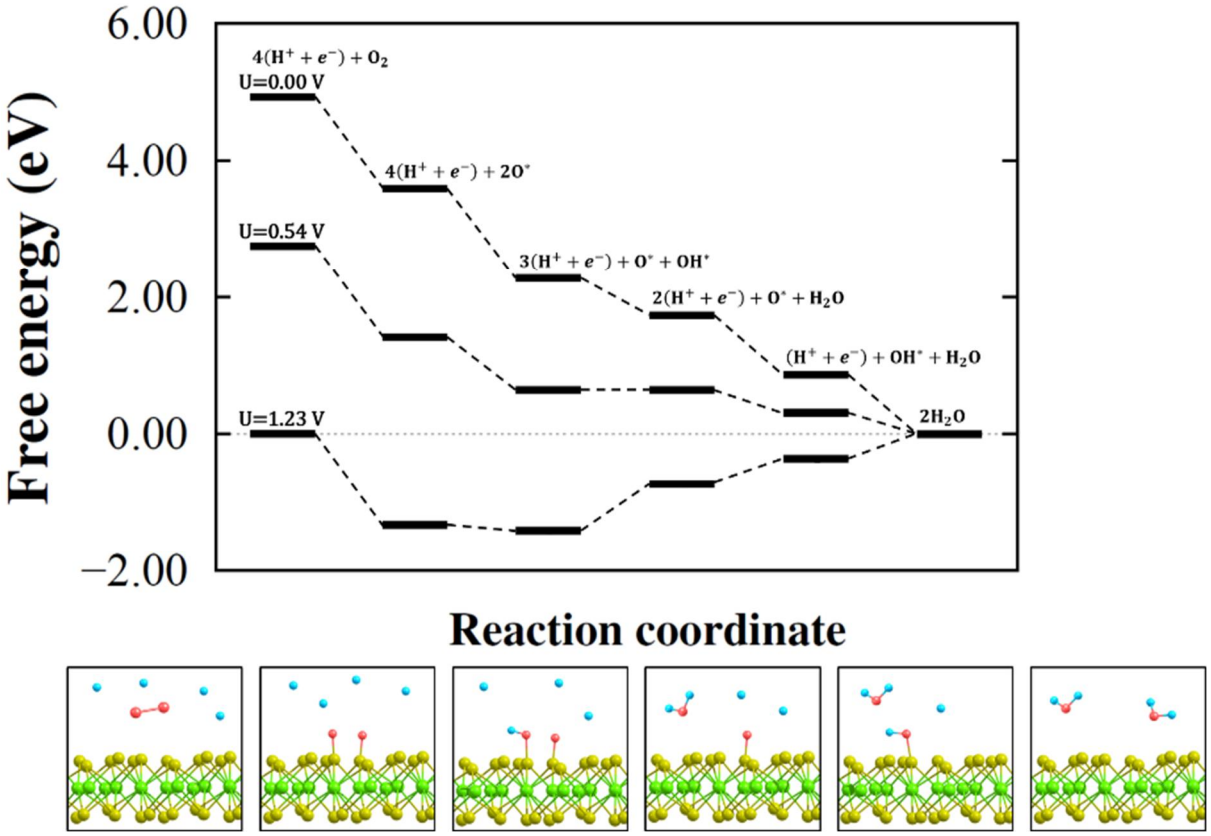

Figure 7 Free-energy profile for oxygen reduction reaction on the charged 1T phase. Results are shown at zero cell potential (U=0V), at the equilibrium potential (U=1.23V), and at the highest potential (U=0.54V) where all reaction steps are exothermic.

List of tables

Table 1 The Results for Bader charge analysis at neutron 1T and charged 1T (2 additional electrons/super-cell).

Bader Charge Analysis	1T	Charged 1T
Before oxygen adsorption		
Mo	+1.254	+1.250
S	-0.6269	-0.6806
O_2	0.00	0.00
After oxygen adsorption		
Mo	+1.237	+1.236
S	-0.5142	-0.5675
O_2	-3.76	-3.81

1. Introduction

Low-dimensional materials, especially transition metal dichalcogenide (TMD), have attracted significant interest these days. The composition of TMD materials is MX_2, where M is transition metal such as Mo and X is chalcogenide molecule such as S. The TMD materials can have two different phases, 2H and 1T, as the stacking positions of chalcogenide molecules. 2H and 1T phase of TMD have trigonal prismatic point group symmetry (D_{3h}) and octahedral point group symmetry (O_h), respectively. Because of these differences of symmetry and the d-orbital splitting of transition metal, TMD materials can show various physical properties such as semiconductor, metal, paramagnetic, antiferromagnetic, and so on.[1,2]

Monolayer MoS_2, one of TMD materials, also shows different physical features as the phases. The 2H phase of MoS_2 is a semiconductor with direct band gap about 2.4 eV, and the 1T phase of MoS_2 has meta-stable metallic phase. The 2H phase of MoS_2 has been studied as a hydrogen evolution reaction (HER) catalyst because of its photovoltaic and photo-catalytic features.[3] On the other hand, the 1T phase of MoS_2 has been investigated in the perspective of nanoscale electronic device, such as ultrathin transistor and supercapacitor electrode component.[4,5,6]

When one electron is injected into the 2H phase of MoS_2, the occupation of E' state of D_{3h} point group is increased. This change of occupation is energetically unstable comparing with the half-filled T_{2g} level of O_h point group. Thus, the phase transition from the 2H phase to 1T phase can occur. Experimentally, Yimin Kang et al. have investigated the phase transition by using the plasmonic hot electron from the deposited Ag nanoparticle on the MoS_2 monolayer.[7] Also, M. A. Py et al. have studied the lithium intercalation method in layered MoS_2 and its phase transition.[8] Goki Eda et al. have observed the structure of mixed phase of MoS_2 by measuring adsorption spectra during lithium intercalation process.[9] They observed the 2H-1T heterophase structure by using high resolution scanning transmission electron microscopy (HR-STEM), and Yung-Chang Lin et al. have investigated the atomic mechanism of this phase transition phenomena.[10,11] Theoretically, Xiaoyan Guo et al. have calculated the electronic properties, especially density of state, of the interface of MoS_2 2H-1T heterophase.[12] However, the detail researches about 2H-1T heterophase such as boundary structure, electron dynamics, and electron transfer between 2H and 1T phase are still unclear.

In this study, we investigated geometric and electronic structure of the MoS_2 heterophase. We found that two different types of phase boundary lead to difference in the band alignments at MoS_2 phase

boundaries. As a consequence, the excited electrons in the 2H phase region are transferred and accumulated in the 1T phase region, leading to the charging of the 1T phase region. We performed the real-time time dependent density functional theory (rt-TDDFT) calculation for this electron dynamics. We found that, as the 1T phase is charged, the activation barrier of dissociative adsorption of oxygen molecule on the planar surface of 1T phase is decreased. In the acidic condition, the oxygen reduction reaction (ORR) energy profile on the charged 1T phase region shows similar electrochemical properties with that on the platinum (100) surface. We suggest that the MoS_2 heterophase can serve as the novel low-dimensional ORR photo-catalyst.

2. Computation Details

A. Electronic and geometric structure

To perform the first-principle calculations, we used the Vienna Ab initio Simulation Package (VASP) source code. For the exchange-correlation potential, a plane-wave basis set with an energy cutoff of 450 eV and the Perdew-Burke-Ernzerhof (PBE) type gradient-correlated functional were employed. The atomic pseudopotentials were described with the Projector Augmented Wave (PAW) method, as provided with the aforementioned package. The heterophase structure was composed with 1x12 rectangular cell of 2H phase and that of 1T phase. The x-direction lattice mismatch between 2H and 1T phase was 0.2%, thus we attached the two rectangular cells along the y-direction. The k-point grids for the heterophase structure were sampled 1x20x1 by using the scheme of the Monkhorst-Pack.

B. Activation energy

The 4x4 1T phase hexagonal supercell with 3x3x1 k-point grids sampling by using the same scheme was employed to investigate the activation barrier of dissociative adsorption of oxygen molecule as the charge accumulation in 1T phase. The nudged elastic band (NEB) method was used to calculate the activation barriers.

C. Oxygen reduction reaction

We assume that $H^+ + e^-$ is in equilibrium with $\frac{1}{2}H_2$, at pH 0 and 0V versus the standard hydrogen electrode (SHE). The free energy of water in the liquid phase was estimated as,

$$G_{H_2O(l)} = G_{H_2O(g)} + RT\ln(\frac{p}{p_0})$$

Where R is the gas constant, T=300K, p=0.035 bar, and p_0=1bar. The free energy of the H^+ ion was derived as

$$G_{H^+(aq)} = \frac{1}{2}G_{H_2(g)} - RT\ln 10 \times \mathrm{pH}$$

In the acidic condition, O_2 is reduced as $O_2 + 4H^+ + 4e^- \rightarrow 2H_2O$, where the elementary reaction steps on the catalytic surface are

1. $O_2(g) + 4H^+(aq) + 4e^- + 2* \rightarrow 2O^* + 4H^+(aq) + 4e^-$
2. $2O^* + 4H^+(aq) + 4e^- \rightarrow O^* + OH^* + 3H^+(aq) + 3e^-$
3. $O^* + OH^* + 3H^+(aq) + 3e^- \rightarrow O^* + H_2O(l) + 2H^+(aq) + 2e^-$
4. $O^* + H_2O(l) + 2H^+(aq) + 2e^- \rightarrow OH^* + H_2O(l) + H^+(aq) + e^-$
5. $OH^* + H_2O(l) + H^+(aq) + e^- \rightarrow 2H_2O(l)$

Where * denotes the free surface, and $H_2O(l)$ indicates liquid water.

3. Result

3.1 Geometric & Electronic Structure

The super-cell what we calculated is consisting of 1x12x1 rectangular cell of 2H and 1T structures. We arranged the rectangular 2H and 1T phase along the y-axis like Figure-1(a), and the lattice mismatch between 2H and 1T phase is 0.42%. The O_h point group, Mo point group of 1T phase, has inversion symmetry while D_{3h} point group, Mo point group of 2H phase, does not. For that reason, there are two different types of boundary, 5-fold and 7-fold coordination number (CN) of transition metal, when the 2H-1T heterophase is formed. Geometrically, the steric effect of 7-fold CN of transition metal is increased because the basal CN of transition metal of TMD materials is 6-fold. In Figure-1(b), therefore, the 7-fold CN boundary has ripple while 5-fold CN boundary is flat.

This change of geometry influences in the electronic structures of the boundaries. When the CN of transition metal is increased from 6-fold to 7-fold, the added chalcogen atom, sulfur for MoS_2 case, increases the oxidation number of transition metal. Thus, the transition metal at the 7-fold CN boundary has more state above the fermi level. On the other hand, the transition metal at the 5-fold CN boundary has less state above the fermi level because the oxidation number of 5-fold CN of transition metal is decreased. For that reason, the electron can be transferred from 7-fold CN boundary to 5-fold CN boundary.

3.2 Excited electron dynamics

We calculated the electron dynamics when photo-excitation occurs at the 2H phase region of aforementioned 2H-1T heterophase structure by using real-time time dependent density functional theory (rt-TDDFT). To decrease the calculating cost for rt-TDDFT calculation, we truncated the 2H-1T heterophase structure in half along the y-axis, so the calculated structure is consisting on the 1x6x1 2H phase and 1x6x1 1T phase. As depicted in the Figure 3, we excite an electron pair from the valance band maximum (VBM) to the conduction band minimum (CBM).

As the schematic configuration in Figure-4(a), the excited electron pair at the 2H phase region is transferred to 1T phase region by passing through the 7-fold CN boundary. Thus, we integrated the charge density at the only 1T phase region by using the following equation,

$$Q_{transferred}(t) = \int_{last\ \mathrm{Mo_{1T}}}^{first\ \mathrm{Mo_{1T}}} \rho(\boldsymbol{r}, t) d\boldsymbol{r},$$

and the transferred charge versus time is plotted in Figure-4(b). The charge density at 1T phase region is increased because the excited charge flows into the 1T phase region via 7-fold CN boundary. As time goes by, the amount of transferred charge has been increased until the excited carrier reaching to the 5-fold CN boundary. After the excited electron passing the 5-fold CN boundary, the amount of transferred charge starts to be decreased. Thus, the retention time for the excited charge staying in the 1T phase region is determined by the size of 1T phase region. For the calculated structure, the 0.4 electrons transferred to 1x6x1 1T phase region, therefore, the $0.067\ electons/_{MoS_{2_{UnitCell}}}$ is transferred from 2H phase region to 1T phase region when the electron pair is excited from the 2H phase VBM.

3.3 Application for oxygen reduction reaction

Aforementioned phenomena represent that the 1T phase region is instantaneously charged when the exciton is generated at the 2H phase region. The charged surface can be utilized for various fields, and the application as the catalyst for oxygen reduction reaction (ORR) is one of them. Several researches have been reported that the charged system or electron applied system such as nitrogen doped graphene or Cabrera-Mott model insulator improve the ORR properties.[13,14] We have studied the ORR properties of the charged 1T phase based on these researches by using DFT calculation.

As described schematic configuration in Figure-5, we calculated the binding energy of oxygen molecule on the 3x3x1 rectangular 1T phase supercell. The oxygen molecule is dissociated and adsorbed on the sulfur atom of 1T phase MoS2, and the binding energy is 0.723eV by following equation,

$$E_{Binding} = \frac{1}{2}\left[E_{MoS_2+O_2} - \{E_{MoS_2} + E_{O_2}\}\right].$$

The oxygen molecule should be dissociative adsorbed on the 1T phase MoS2 thermodynamically, however that phenomena does not be happened in real. Thus, we calculated the activation energy for dissociative adsorption ($E_{a_{diss}}$) by using the nudged elastic band (NEB) method as implemented with the VASP code, and considered the kinetical component based on the Arrhenius type reaction rate.

As depicted in Figure-6, the $E_{a_{diss}}$ on the basal 1T phase is about 2.5eV, and it is extremely high barrier comparing with Boltzmann factor at room temperature, about 0.026eV. However, $E_{a_{diss}}$ is decreased dramatically when the ORR system is charged. Especially, the $E_{a_{diss}}$ is decreased to 0.05eV when $0.067\ electons/_{MoS_{2_{UnitCell}}}$, the result of our rt-TDDFT calculation, is charged at the 1T phase.

Also, we calculated the Bader charge analysis to study the reason why $E_{a_{diss}}$ is dramatically decreased as the additional charge. As the Table-1 shown, the charge at molybdenum atom is not changed when the excess charge is injected. The charge at sulfur atom, however, is increased as same amount of the excess charge. The charge at molybdenum atom is still not changed when oxygen molecule is adsorbed while the charge at sulfur atom is decreased. That is, the excess charge deposits in only sulfur atom, the outer layer of MoS_2, and that charge transfers to oxygen molecule for dissociative adsorption. Therefore, the electron affinity of oxygen molecule helps to decrease $E_{a_{diss}}$ by being dragged to the charged surface of MoS_2.

Herein, we utilize the dissociative adsorbed oxygen molecule on the 1T phase MoS_2 as following steps

for 4-electron the ORR mechanism.

$O_2 + 4H^+ + 4e^- \rightarrow 2O^* + 4H^+ + e^-$

$2O^* + 4H^+ + 4e^- \rightarrow O^* + HO^* + 3H^+ + 3e^-$

$O^* + HO^* + 3H^+ + 3e^- \rightarrow O^* + H_2O + 2H^+ + 2e^-$

$O^* + H_2O + 2H^+ + 2e^- \rightarrow HO^* + H_2O + H^+ + e^-$

$HO^* + H_2O + H^+ + e^- \rightarrow 2H_2O$

Based on the standard hydrogen electrode, the potential for oxygen molecule reduction, $O_2 + 4H^+ \rightarrow 2H_2O$, is 1.23V when the potential for protonation of hydrogen molecule is 0V. In the Figure-7, the free-energy diagram by calculating the potentials for each electron transfer step based on the free-energy calculation method of Norskov et al. shows that the potential profile has downhill until overpotential, μ, is 0.54V, and after that the potential profile has uphill.[15] That is, the current has not been changed until the bias potential reaching from 0V to 0.54V. But after the μ over the 0.54V, the current is decreased because of uphill at the free-energy diagram following the Butler-Volmer equation,

$i_k = i_0 e^{(U/kT)}$.

4. Conclusion

The 2H-1T heterophase can has two-type boundaries as the CN of transition metal at the boundary. The CN of transition metal can influence in the geometric and electronic structure of that heterophase, and it decides the direction of electron transfer from 2H phase to 1T phase. The amount of transferred electron is $0.067\ electons/_{MoS_{2\,UnitCell}}$ and it's enough to attract oxygen molecule onto the 1T phase of MoS_2 with extremely decreased adsorption activation energy. The dissociative adsorption of oxygen molecule is rate determine step (RDS) for ORR mechanism, and this photovoltaic effect at 2H phase of MoS_2 supports to improve the ORR properties on the 1T phase of MoS_2. Our results of free-energy diagram shows that the maximum overpotential where the proton transfer step is down-hill in energy is 0.54V. Experimentally, the ORR property, especially i-v curve data, on Pt (100) surface shows similar result with ours.[16] From our simulation results, the electron transfer from 2H, the semiconductor phase, to 1T, the metallic phase, by photovoltaic effect can improve the ORR property and it be utilized as the photo-catalyst for ORR.

REFERENCES

1. Manish Chhowalla, Hyeon Suk Shin, Goki Eda, Lain-Jong Li, Kian Ping Loh, and Hua Zhang; Nature Chemistry (2013) vol 5 263-275

2. Andrey N. Enyashin, Lena Yadgarov, Lothar Houben, Igor Popov, Marc Weidenbash ReshefTenne, Maya Bar-Sadan, and Gotthard Seifert; The Journal of Physical Chemicsry C (2011) 155, 24586-24591

3. Haotian Wang, Zhiyi Lu, Shicheng Xu, Desheng Kong, Judy J. Cha, Guangyuan Zheng, Po-Chun Hsu, Kai Yan, David Bradshaw, Fritz B. Prinz, and Yi Cui; Proceeding of th eNational Academy of Sciences of the United States of America (PNAS) (2013) 110, 19701-19706

4. Muharrem Acerce, Damien Voiry, and Manish Chhowalla; Nature Nanotechnology (2015) 10, 313-318

5. Xiao Huang, Zhiyuan Zeng, and Hua Zhang; Chem. Soc. Rev. (2013) 42, 1934-1946

6. Rajesh Kappera, Damien Voiry, Sibel Ebru Yalcin, Brittany Branch, Gautam Gupta, Aditya D. Mohite, and Manish Chhowalla; Nature Materials (2014) vol 13 1128-1134

7. Yimin Kang, Sina Najmaei, Zheng Liu, Yanjun Bao, Yumin Wang, Xing Zhu, Naomi J. Halas, Peter Nordlander, Pulickel M. Ajayan, Jun Lou, and Zheyu Fang; Advanced Materials (2014) 26 6467-6471

8. M. A. Py, R. R. Haering; Canadian Journal of Physics (1983) 61, 76-84

9. Goki Eda, Hisato Yamaguchi, Damien Voiry, Takeshi Fujita, Mingwei Chen, and Manish Chhowalla; Nano Letter (2011) 11, 5111-5116

10. Goki Eda, Takeshi Fujita, Hisato Yamaguchi, Damien Voiry, Mingwei Chen, and Manish Chhowalla; ACS Nano (2012) vol 6 7311-7317

11. Yung-Chang Lin, Dumitru O. Dumcenco, Ying-Sheng Huang, and Kazu Suenaga; Nature Nanotechnology (2014) vol 9 391-396

12. Xiaoyan Guo, Guihui Yang, Junfeng Zhang, and Xiaohong Xu; AIP Advances (2015) 5, 097174

13. Linfer Lai, Jeffrey R. Potts, Da Zhan, Liang Wang, Chee Kok Poh, Chunhua Tang, Hao Gong, Zexiang Shen, Jianyi Lin, and Rodney S. Ruoff; Energy Envitonment Science (2012) 5, 7936-7942

14. Dongbin Shin, S. Sinthika, Min Choi, Ranjit Thapa, Noejung Park; ACS Catalyst (2014) 4, 4074-4080

15. Origin of the Overpotential for Oxygen Reduction at a Fuel-Cell Cathode
J.K. Norskov, J. Rossmeisl, A. Logadottir, L. Lindqvist, J. R. Kitchin, T. Bligaard, and H. Jonsson; J. Phys. Chem. B (2004) 108, 17886-17892

16. N.M.Markovic, P.N.Ross Jr.; Surface Science Reports 45 (2002) 117-229